

Morphology, Structure and Nonstoichiometry of ZnCr_2O_4 Nanophased Powder

L.Mancic^{1,*}, Z.Marinkovic², P.Vulic³, C.Moral⁴ and O.Milosevic¹

¹Institute of Technical Sciences of Serbian Academy of Sciences and Arts, Knez Mihailova 35/IV, 11000 Belgrade, Serbia-Montenegro. Tel/Fax +381 11 637239

²Center for Multidisciplinary Studies, University of Belgrade, Kneza Visislava 1a, 11 000 Belgrade, Serbia-Montenegro

³Faculty of Mining and Geology, Department of Crystallography, Djusina 7, 11000 Belgrade, Serbia-Montenegro

⁴University Carlos III, Avda.de la Universidad 30, 28911 Leganes, Madrid, Spain

* Author to whom correspondence should be addressed: lydia@itn.sanu.ac.yu

Received: 15 May 2003/ Accepted: 17 August 2003 / Published: 31 October 2003

Abstract: It is well established that gas/humidity-sensing properties of spinels are markedly influenced by their stoichiometry and microstructure. In this work nucleation and spinel phase development in the Zn-Cr-O system were investigated from the viewpoint of structural and morphological phenomena occurred during nanophased particle synthesis through aerosol reaction. The aerosol was generated from nitrates precursor solution using ultrasonic atomizer operated at 1.7 MHz. The influence of different decomposition schedules on the particle chemical content and morphology was determined by adjusting the processing parameters (aerosol droplet density 3.9×10^6 droplets/cm³, droplet velocity 0.035m/s, max. temperature 900°C and residence times 3, 6 and 9s). A composite particle structure comprised of primary crystallites sized from 22 to 44nm is revealed by SEM and TEM analysis. XRD structural analysis (crystallite size, microstrains, unit cell and ionic occupancies) is performed in accordance with procedure based on Koalariet-Xfit program. A certain degree of non-stoichiometry is characteristic for all powders. Homogenous distribution of the constituting elements and Zn/Cr ratio of about 0.68 are proved by EDAX

mapping analysis in 470nm sized as-prepared particles. After additional treatment at 1000°C octahedral crystals form with the (111) surface dominant. Evaluated spinel non-stoichiometry ($Zn/Cr=0.58$) is a result of the ZnO dissolving (1.9%wt) in the stoichiometric $ZnCr_2O_4$. Determination of the way by which the ZnO is incorporated into the spinel lattice is performed according to the procedure based on calculation of both formation and attachment energies.

Keywords: Spray pyrolysis, nanostructure, nonstoichiometry, $ZnCr_2O_4$.

Introduction

Amongst the various types of solid-state humidity sensors that have been proposed in the literature the simplest are sensors which use solid electrolytes or semiconductors as the active elements [1,2]. A ceramic material seems to be more appropriate as active elements, given that they are thermally and chemically stable, reliable and selective [3].

Oxides with the spinel structure are some of the most studied compounds in solid-state sciences due to their wide range of applications. The structure of spinel oxide is responsible for a variety of interesting properties [2-6]. Determination of cation distribution is of considerable relevance because the theoretical interpretation of the chemical and physical properties of these compounds depends on this distribution [5]. In order to understand how a ceramic material interacts with its environment, it is necessary to determine the atomic structure at its surface [7].

$ZnCr_2O_4$ is expected to have sufficient thermodynamic stability and perfect sensing properties, but its possible use as humidity-sensing material have never been fully exploited. It was expected that a well-defined microstructure should be formed in order to improve the humidity sensitive properties [2,6-8].

A detailed investigation of the microstructure evolution of the nanophased spinel $ZnCr_2O_4$ powder prepared by aerosol synthesis is reported in this article.

Experimental

$ZnCr_2O_4$ spinel was synthesized according to a previously described method [4]. The precursor solution for atomization was prepared by dissolving the appropriate amounts of corresponding metal nitrates $Zn(NO_3)_2 \cdot 6H_2O$ and $Cr(NO_3)_3 \cdot 9H_2O$ in distilled water, in order to obtain 0.03 mol/dm^3 . Assuming that the precursor stoichiometry persisted in the final particles, a Zn:Cr = 1:2 cations ratio is chosen for the starting composition. The aerosol was produced by an ultrasonic generator (Gapusol RBI, 1.7 MHz) and introduced in a twin-zone tubular flow reactor with air as the carrier gas. The heated region was a 1.3 m long, 3.2 cm dia quartz tube, with increase-humped temperature profile and $T_{\text{max}}=900^\circ\text{C}$ in both reaction zones. Three charges of powders were collected with different droplet/particle residence time - after the first heated zone (powder charge 1), the second one (powder charge 2) and from the collecting chamber (powder charge 3). In the case of powder charge 1, the aerosol residence time was 3s at T_{max} . After the powder was trapped, hot air (700°C) blow over the

powder sample for an additional 16 h. The residence time for powder charge 2 at T_{\max} was 6s. Similarly as for the charge 1, after the powder charge 2 was trapped, hot air (400°C) blow over the powder sample for an additional 16 h. Powder charge 3 had a residence time of 9s at T_{\max} . The temperature in the collecting chamber was 150°C. All the as-prepared samples were checked by powder XRD. As-prepared powders were additionally thermally treated at a temperature of 1000°C for 2 hours.

The investigation of precursors decomposition behavior was examined by differential scanning calorimetry (detector type SHIMADZU DSC-50) under a nitrogen atmosphere at a heating rate of 10°C/min.

Particle size distribution analysis was carried out with a Malvern Laser Master Sizer. 100mg of as-prepared powders were used for analysis, ultrasonically deagglomerated and suspended in referent solution (0.05% sodium hexametasulphate water solution).

X-ray diffraction data of thermally treated powders were collected in the range 3°-70° (2 θ), using a Philips PW 1710 automated diffractometer with $\text{CuK}\alpha$ radiation and a graphite monochromator. Step-scanning was 0.02°/15s. All peak positions were used in the determination of precise microstructural parameters. Structural refinements were carried out using the Rietveld program Koalariet-Xfit [9]. Peak profiles were fitted with a pseudo-Voight function and asymmetry parameters were considered for peaks below 70° (2 θ). The background was refined with a polynomial function.

Compositional homogeneity and morphology of obtained particles were determined in accordance to scanning/transmission electron microscopy (SEM S-4500), TEM (JEOL JEM-200) and HORIBA X-ray Microanalyzer EMAX-7000. For that purpose, powder samples were sputtered with Au (Au depth layer 150 A made by Quick auto Coater JFC 1500). Qualitative and quantitative sample analysis were proceeded in accordance to spot (analyzing area 100A, beam depth 50 nm) as well as square analysis. Mapping of the constitutive elements was proceeded for the purpose of inner particle uniformity confirmation.

Results and Discussion

Thermal analysis of mixed precursor salts shows that precursor decomposition is complete at a temperature below 350°C [4]. Having in mind specific mechanisms of particle formation during the spray pyrolysis process, as well as the fact that spinel phase formation during conventional solid-state reaction process occurs at temperatures higher than 1000°C [8], a temperature of 900°C is chosen as a maximum temperature for the synthesis process.

Particle size measurements, performed for all investigated samples, show the same value of mean particle size, estimated to be 470nm, indicating that residence time did not affect a broadening of the particle size distributions [4].

From the SEM micrographs on Fig.1 is easy to notice morphology changes that occurred with increasing residence time. Having in mind that powders from charges 1 and 2 were exposed to *in situ* additional thermal treatment at different temperatures (since they were trapped in tubular furnace after first and second zone during synthesis) powder from charge 3 is characterized with the shortest residence time (9s on T_{\max} , 38s in tubular furnace).

The main feature of particles presented in Fig.1c is their composite structure and the presence of primary crystallites visible on their surface. Two types of particles are setting apart. While some of them have visually uniform surface composition, others are characterized by compositional segregation limited to the level of primary grains. For the powders from charge 1, shown in Fig.1a (3s on T_{max} , additional 16h on 700°C), characteristic smooth surface of the individual irregular shaped particles indicating dense particle formation with a crust evolved during the melting of the precursor. Particle bonding and neck formation denote initial interparticle sintering. Slightly agglomerated particles from charge 2, Fig.3b (6s on T_{max} , additional 16h on 400°C), exhibit the coexistence of both smooth, dense particles, as well as composite ones, having complex inner crystallite structure.

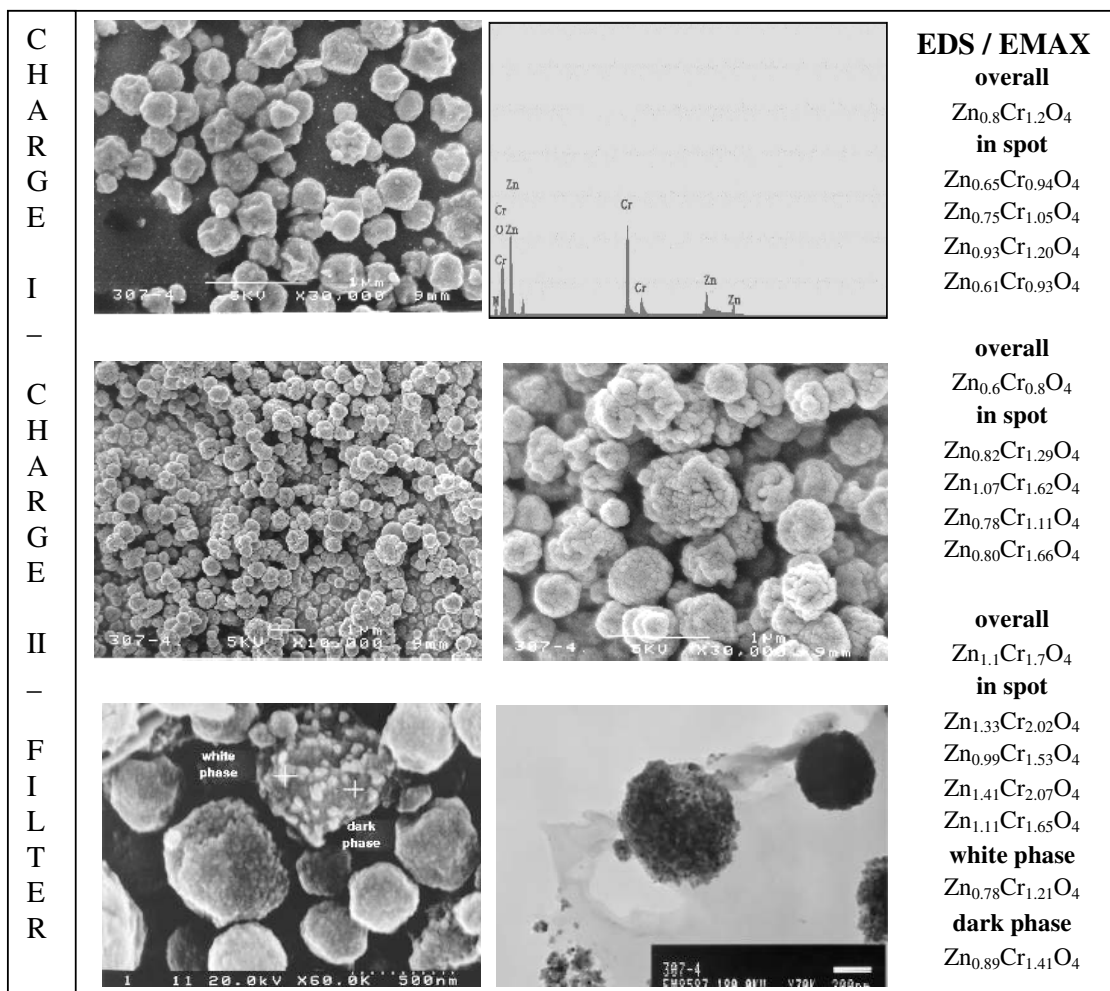


Fig.1 Scanning electron micrographs of the as-prepared $ZnCr_2O_4$ powders:

a) charge 1; b) charge 2; c) charge 3

EMAX mapping for as-prepared samples showed uniform distribution of the constitutive elements inside the examined particles: zinc, chromium, oxygen and nitrogen [4]. The results obtained mean that during spray pyrolysis each particle is formed through volume precipitation. This is proved also by

TEM analysis, Fig.1. The primary crystallites visible on Fig.1 ranged from 10 to 60nm, which is in accordance with diffraction line broadening analysis(Table1.).

Chemical composition determined by semiquantitative EMAX analysis indicates similar stoichiometry for all examined particles, with the mean Zn/Cr ratio at 0.68. The value obtained denotes the solution concentration ratio (0.5) is not fully achieved in the resulting particles, while the presence of nitrogen should be the consequence of the high reactivity of synthesized powders and also surface chemisorption. Considering the obtained particle stoichiometry, no clear evidence about the influence of the particle residence time on the Zn/Cr concentration ratio was established.

Together with SEM/EMAX morphological analysis, XRD data have also allowed a better characterization of the chemical homogeneity of the as-prepared powders. A typical X-ray diffraction pattern of as-prepared powders is presented on Fig.2a. Spinel phase (ZnCr_2O_4) formation is confirmed in all investigated samples due to the presence of diffraction lines indicated on the JCPDS cards 22-1107 (8.327 Å). Slightly broadening of diffraction lines may be attributed to small crystallite effects, crystal defects or chemical heterogeneity of the samples. In accordance with the procedure based on Koalariet-Xfit program [9], results of structural refinement obtained for as-prepared spinel powders are present in Table 1. Considering Zn^{2+} and Cr^{3+} cation radii the spinel phase with higher unit-cell parameter (a) should be richer in Zn. It is not possible to establish the influence of the primary crystallite size and microstrains change versus particle residence time by comparison the attained structural parameters given in Table 1, but the same behavior in changes is observed.

Table 1. Values of lattice parameters (a), average crystallite size (D) and crystal lattice microstrains (ϵ) in as-prepared ZnCr_2O_4 particles

Powder charge	a [Å]	D [nm]	$\langle \epsilon^2(L) \rangle^{1/2}$ [%]
1	8.332±0.001	33.3±3.1	0.551±0.068
2	8.338±0.001	22.6±1.2	0.125±0.054
3	8.335±0.001	44.1±6.4	0.638±0.081

Determined cation ratio in as-prepared spinel powders at 0.68 confirmed presumptions that the residence time of each droplet/particle is insufficient to fully establish the stoichiometry dictated by the precursor solution. The condition which have ensured further diffusion of Cr^{3+} cations into previously formed spinel crystal lattice include an additional thermal treatment of as-prepared powders. The powder diffraction data of the ZnCr_2O_4 samples annealed at 1000°C shown in Fig.2b, reveal a well-crystallized cubic spinel phase (98.1 wt%). Also, a small amount (1.9 wt%) of ZnO phase (JCPDS cards 36-1451) was detected. The occupancy values of particular cation sites in the spinel crystal lattice (Zn^{2+} -0.9951; Cr^{3+} -0.9593) correspond to the spinel phase with the cation Zn/Cr ratio of 0.52. Estimated values of structural refinement such as unit-cell parameters (a , b), average crystallite size (D) and crystal lattice microstrains (ϵ) of obtained phases after heating are presented in Table 2.

The presence of ZnO as an accompanying phase in the process of spinel synthesis, is known. Although, non-stoichiometry of spinel compound due to the dissolution of excess oxide which containing three valent ions (in our case Cr_2O_3) is more typical [8]. In addition, there is also the possibility of forming Schottky defects and three kinds of Frenkel defect at high temperatures.

Stoichiometric ZnCr_2O_4 has a face-centered cubic arrangement of oxygen ions space group $\text{Fd}\bar{3}\text{m}$, in which the Cr^{3+} ions occupy half of the octahedral and the Zn^{2+} ions fill one-eighth of the tetrahedral

Table 2. Structural parameters of obtained phases ZnCr_2O_4 and ZnO in powder charge 1 after additional heating

Phase	Unit-cell parameter, Å	D, nm	ϵ , %
ZnCr_2O_4	8.330 ± 0.001	337.7 ± 18	0.0647 ± 0.003
ZnO	a=b: 3.251 ± 0.001 c: 5.207 ± 0.001	388.1 ± 13	0.0472 ± 0.019

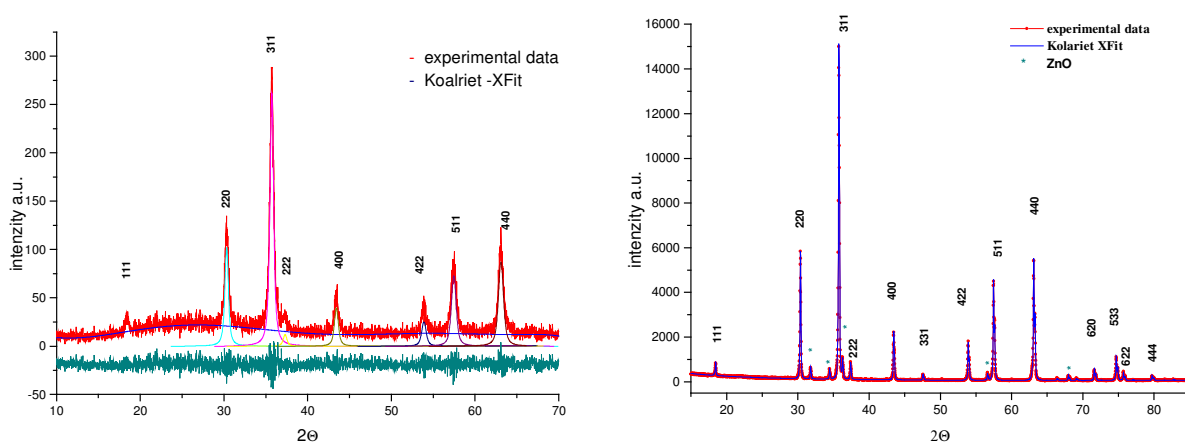


Fig. 2 Experimental and calculated diffraction profiles obtained for as-prepared (a) and thermally treated (b) ZnCr_2O_4 powder (charge 1)

sites enclosed within the anion sublattice. With this distribution, the theoretical calculated lattice parameter of the crystal is 8.340Å . The variation in the experimental values, in the range $8.321\text{--}8.359\text{Å}$ [8,10,11], may indicate formation of a non-stoichiometric and defective material. It is shown that atomistic methods for simulation and description of the perfect and defect spinel ZnCr_2O_4 crystal lattice based on the calculation of the formation energies of an ideal crystal, as well as set of isolated defects and also defects cluster formation could be used for the interpretation of this variation [8]. According to this model, the different defect reactions associated with ZnO solution give rise to different combinations of defects. Two of them lead to a decrease of lattice parameter, while others result in an increase of the spinel unit cell, see Fig.3. Together with the predicted lattice parameters from model [8] the experimental data presented in this study are shown on the same figure (lattice parameters from Koalriet –Xfit structure refinement* and Zn content determined through EDS/EMAX analysis) indicating that clustered Cr^{4+} defects are the dominant defects present in prepared spinel structures of nanophased powders.

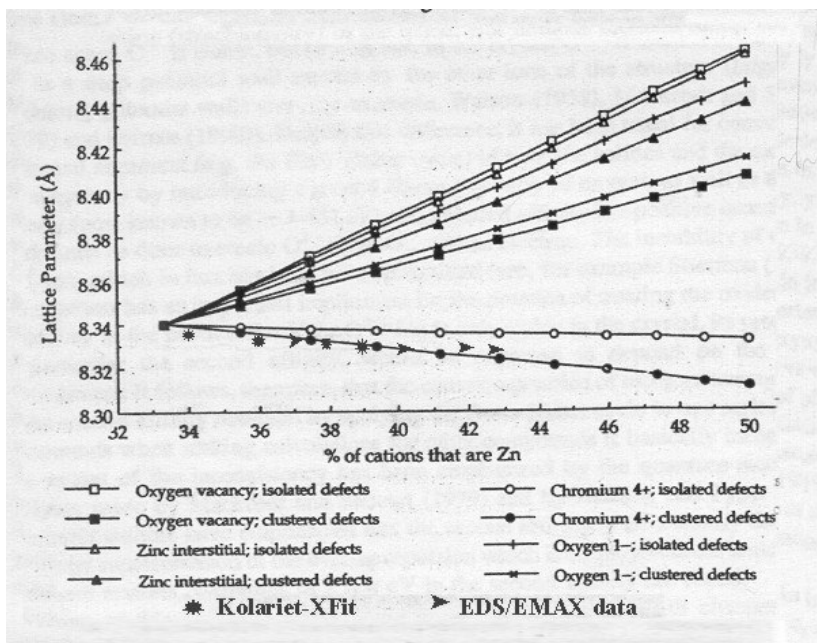


Fig. 3 Predicted spinel lattice parameters due zinc excess presence [8] shown together with the experimental data presented in this study (* Kolariet-Xfit; ▶EDS/EMAX)

The same authors also used their description of the interactions between ions during spinel formation to predict the resultant crystal morphology of ZnCr_2O_4 [7]. In this study crystallites are predicted to be essentially octahedral with the (111) surface dominating, stabilized by the presence of defects on surfaces. Shapes of the crystallites could be determined by two separate methods based on attachment and surface energies calculation, see Fig.4a-d. SEM micrographs of powders after thermal treatment presented in the same figure confirms that the observed particle morphology is one of those predicted (Fig.4b) that is associated with the calculation based on the growth of a highly defect surface structure. This relaxed growth mode was controlled by the slowest growing surface (111) in combination with tiny cups originated from (220) planes.

This significant microstructural and morphological change observed through the development of octahedral forms with the base under $1\mu\text{m}$ dominate the crystallite morphology. In addition, spherical particles and irregular shaped aggregates, which additionally densify during thermal treatment, are visible too, Fig.4.

Conclusion

The aerosol decomposition processes have been carried out in the temperature range up to 900°C with various droplet/particle residence times, with the purpose of ZnCr_2O_4 spinel phase synthesis. Slightly agglomerated, 470nm sized spherical particles with a homogenous distribution of constitutive elements and a Zn/Cr cation ratio of 0.68 were obtained irrespective with the residence time. A complex particle structure proved by the existence of primary crystallites sized from 22 to 44nm is revealed for the as-prepared powders, while additional heat treatment leads to increasing primary

crystallites sizes up to 338nm. The experimental results obtained are in excellent agreement with model calculations which predict an excess of Zn^{2+} present in the spinel lattice compensated by Cr^{4+} ions. The excess Zn^{2+} and Cr^{4+} ions are associated defect clusters. Additionally, the achieved morphology and shape of the spinel crystallites in thermally treated powders supported the predicted morphology based on calculation of attachment energy with (111) surface domination.

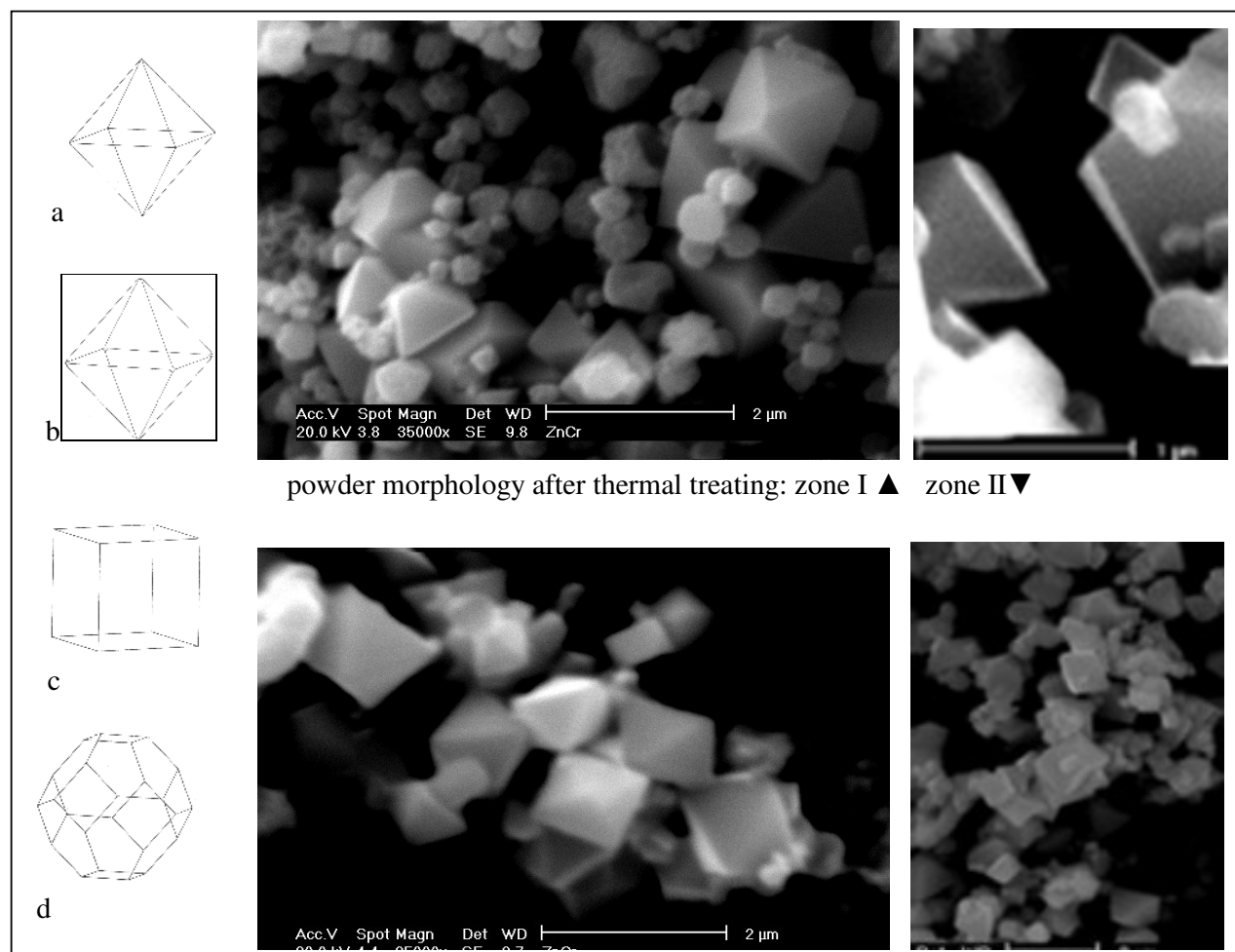


Fig. 4. Predicted morphology of spinel crystals according to model [6] using: a) unrelaxed and b) relaxed attachment energies; c) unrelaxed and d) relaxed surface energies. Typical particle morphology of powders charge 1 and charge 2 after additional heat treatment

Acknowledgements

This research was financially supported by the Ministry of Science Technology and Development, Republic of Serbia through the project No.1832 (Synthesis of functional materials from the viewpoint of synthesis-structure-properties-application relationship), as well as NEDO International Joint

Research Grant Program No.01MB7 (Wettability of solid by liquid at high temperatures). Authors are grateful to prof. R.W.Grimes for using a part of his results at Fig.3 in this work.

References and Notes

1. Fagan J.G.; Amarakoon V.R.W; Reliability and reproducibility of ceramic sensors: Part. III. Humidity sensors. *Am. Ceram. Soc. Bull.*, **1993**, 72,119-129.
2. Yokomizo Y.; Uno S.; Hirata M.; Hiraki H. Microstructure and humidity- sensitive properties of $ZnCr_2O_4$ - $LiZnVO_4$ ceramics sensors. *Sens.Actuators*, **1983**, 4, 599-606.
3. Nitta T.; in Chemical sensor technology, vol. 1, ed. by T.Seiyama. Kodansha-Elsevier, New York, **1988**, 57
4. Marinkovic Z.V.; Mancic L.; Maric R.; Milosevic O. Preparation of nanostructured Zn-Cr-O spinel powders by ultrasonic spray pyrolysis. *J.Euro.Ceram.Soc.* **2001**, 21, 2051-2055.
5. Ferreira T.A.S.; Waerenbourgh J.C.; Mendonca M.H.R.M.; Nunes M.R.; Costa F.M.; Structural and morphological characterization of $FeCo_2O_4$ and $CoFe_2O_4$ spinels prepared by a coprecipitation method. *Solid State Sciences* **2003**, 5, 383-392.
6. Pokhrel S.; Jeyaraj B.; Nagaraja K.S.; Humidity-sensing properties of $ZnCr_2O_4$ -ZnO composites. *Mater. Lett.* **2003**, 4378, 1-6.
7. Binks D.J.; Grimes R.W.; Rohl A.L.; Gay D.H.; Morphology and structure of $ZnCr_2O_4$ spinel crystallites. *J. Mater. Sci.* **1996**, 31,1151-1156.
8. Grimes, R.W.; Binks D.J.; Lidiard A.B. The extent of zinc oxide solution in zinc chromate spinel. *Philosophical Magazine* **1995**, 72(3), 651-668.
9. Cheary R.W., Coelho, A.A., Programs XFIT and FOURYA, CCP14 Powder diffraction Library-Daresbury Laboratory, Warrington, England, **1996**.
10. Leccabue F.; Pelosi C.; Agostinelli E.; Fares V.; Fiorani D.; Paparazzo E.; Crystal growth, thermodynamical and structural study of $CoGa_2O_4$ and $ZnCr_2O_4$ single crystals. *J.Cryst.Growth.* **1986**, 79, 410-416.
11. Dabkowska H.; Flux growth of $CdCr_2O_4$ and $ZnCr_2O_4$ single crystals by the slow cooling method from different fluxes. *J.Cryst.Growth.* **1981**, 54, 607-609

Sample Availability: Available from the authors.

© 2003 by MDPI (<http://www.mdpi.org>). Reproduction is permitted for noncommercial purposes.